Numerical description of surface flows at the hillslope scale

Stefano Orlandini[1] Giovanni Moretti[1]
John D. Albertson[2]

[1]Dipartimento di Ingegneria "Enzo Ferrari," Università degli Studi di Modena e Reggio Emilia, Modena, Italy

[2]Department of Civil and Environmental Engineering, Duke University, Durham, North Carolina, USA

Presentazione dei Risultati dei Progetti PRIN 2008
Università degli Studi di Ferrara, 24 e 25 Gennaio 2013

Analysis of flow and transport processes at the hillslope scale
Coordinatore scientifico: Aldo Fiori, Università degli Studi Roma Tre

Outline

Overland flow phenomenology and modeling.

- Surface and subsurface flows interact along hillslopes and channels by affecting:
  - Runoff production mechanisms. CATHY
  - Solute and sediment transport.
  - Land stability.
- The phenomenology of the overland flow is known (e.g., Raudkivi, 1979, p. 170 and 171). Overland flow phenomenology
- Overland flow models are, however, poorly validated against field observations.
- Released hydrographs are generally inadequate to investigate hydrologic interactions inside the drainage basins (e.g., surface-subsurface, hillslope-channel, soil-vegetation-atmosphere, etc).

Where does overland flow occur?
Sensitivity and specificity issues.

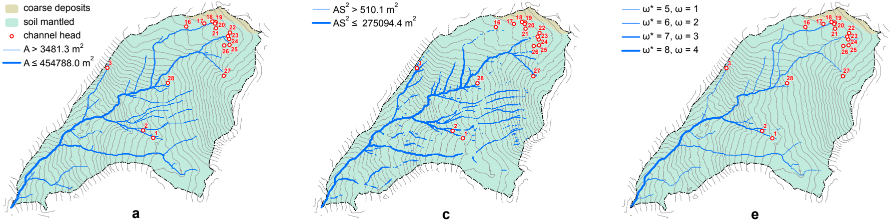

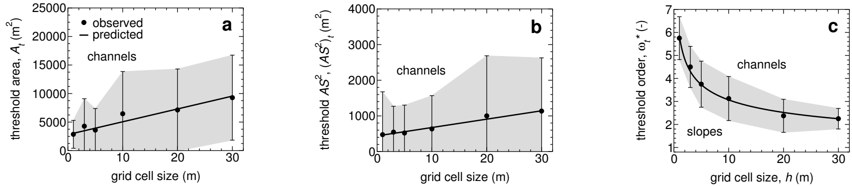

(Orlandini et al., 2011, WRR)

How is land surface topography characterized?

Contour-based terrain analysis models

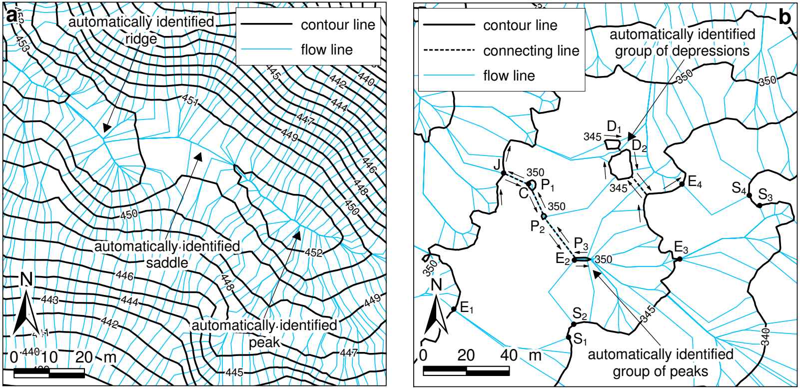

(Moretti and Orlandini, 2008, WRR) Skeleton

Slope and flow lines

How is land surface topography characterized?

Triangulated irregular networks

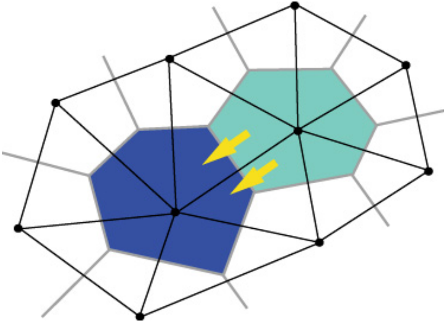

(Ivanov et al., 2004, WRR)

How is land surface topography characterized?

Grid-based terrain analysis models

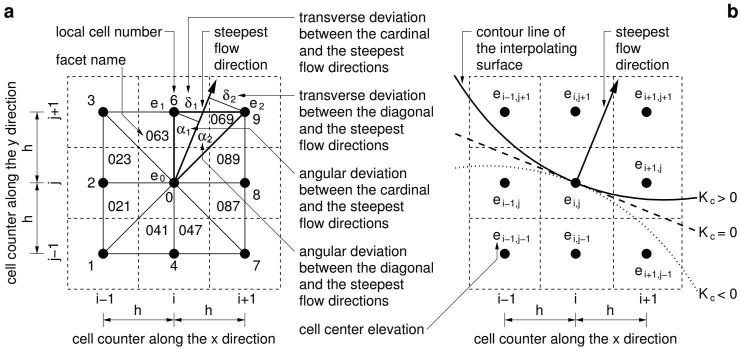

(Orlandini and Moretti, 2009, WRR)

Methods: D8, MD8, D∞, D8-LTD, MD∞, and D∞-LTD. ▸ LTD
(2-D/D4 propagation across adjacent cells may not be robust.)

Are profile and planar dispersion are relevant factors?

Profile/hydraulic dispersion

$$\frac{\partial Q}{\partial t} + c_k \frac{\partial Q}{\partial s} = D_h \frac{\partial^2 Q}{\partial s^2} + c_k\, q$$

$$c_k = \frac{dQ}{d\Omega}$$

$$D_h = \frac{Q}{2\, W\, S_0}\left(1 - \mathrm{Ve}^2\right)$$

$$\mathrm{Ve} = (c_k - U)/\sqrt{g\, Y_m}$$

$$D_n = c_k\, \Delta s \left(\frac{1}{2} - X\right)$$

Planar dispersion

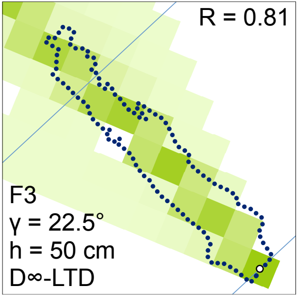

Cell shades indicate the fraction of released water passing through the cell.

Green is the colour of her kind
quickness of the eye deceives the mind
(Pink Floyd, Green is the Colour, More, 1969)

Line source on impermeable bedrock slope.

Experiment setup.
(Orlandini et al., 2012, WRR)

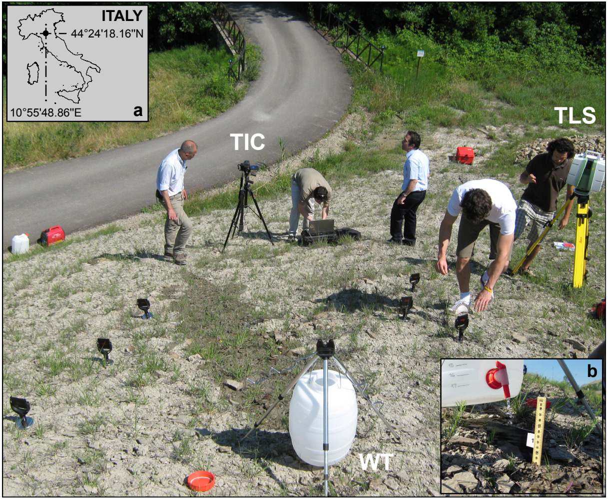

Underlaying philosophy.

- It is a general philosophy in studies of environmental fluid mechanics to begin with the most fundamental and general, such as point sources, and to study the subsequent dispersion and transport. This investigation is presented in this way, and as in the classic studies of turbulent dispersion the line of inquiry should then proceed to line sources, grid sources and so on.
- In the flow direction methods considered, a drainage area which originates over a two-dimensional cell is treated as a point source (nondimensional) and is projected downslope by a line (one-dimensional). There is, therefore, consistency between the considered flow patterns and the considered predictions.
- The philosophy of the present investigation is to consider the observed data in a purely direct manner, with minimal processing (and potential contamination) of these data, in order to provide an objective evaluation of methods and to identify directions for future research.

Technical specifications.

- Date of the experiment: June 2010.
- Slope: soil composed of clay and small stones.
- Terrain slope: approximately 50%.
- Experiment: cold (2–10°C) water released on the warmer (15–30°C) dry land surface.
- Flow discharge released: 8.9, 9.6, and 18.9 cm^3 s^{-1} (for the F1, F2, and F3, respectively).
- Flow duration: 29.1, 32.2, and 15.5 min (for the F1, F2, and F3, respectively).
- Flow velocities: approximately 2.6×10^{-3}, 3.4×10^{-3}, and 5.6×10^{-3} m s^{-1} (for the F1, F2, and F3, respectively).

Technical specifications.

- Terrestrial laser scanner: ScanStation C10 platform by Leica Geosystems.
- Scan rate: up to 50,000 points per second.
- Point cloud densities: 26, 28, and 21 points/cm^2 (for the F1, F2, and F3, respectively).
- Thermal imaging camera: Avio Advanced Thermo TVS-500EX camera by Nippon Avionics.
- Maximum acquisition frequency: 60 frames per second.
- Temperature resolution: better than 0.05°C.

Land reflectance and temperature images.

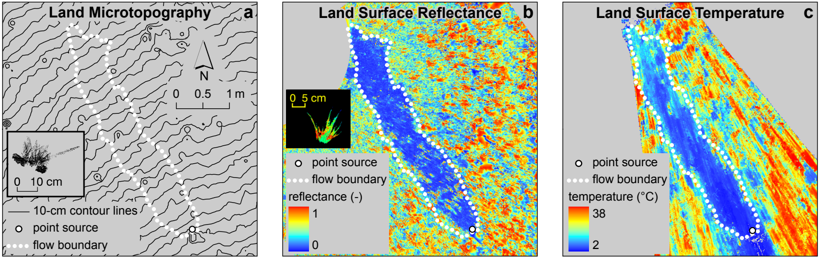

I'm coming up on infra-red, there is no running that can hide you,
'Cause I can see in the dark.
I'm coming up on infra-red, forget your running, I will find you.
(Placebo, Infra-red, Meds, 2006)

Are predicted flow patterns affected by size of grid cells?

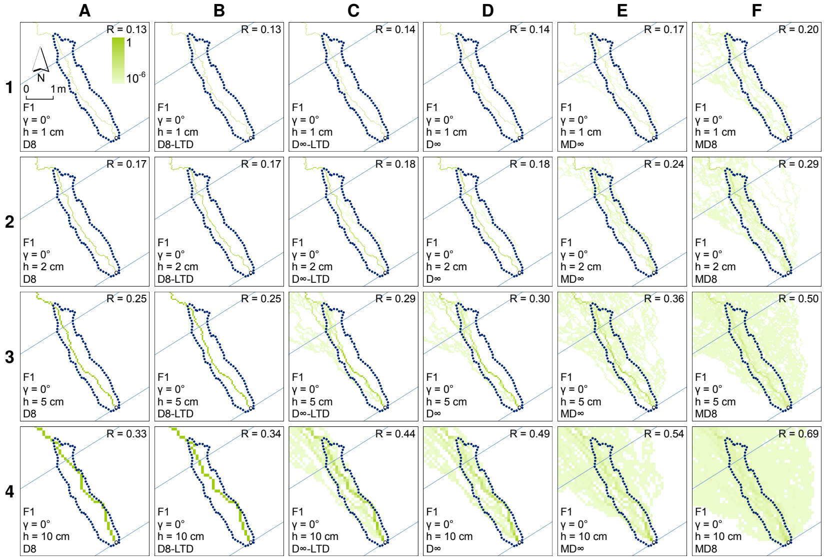

Are predicted flow patterns affected by size of grid cells?

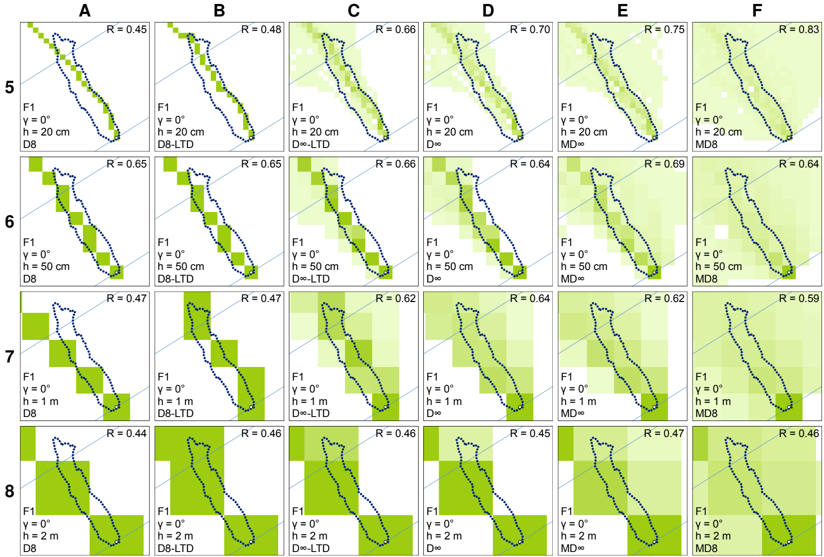

Are predicted flow patterns affected by orientation of grid cells?

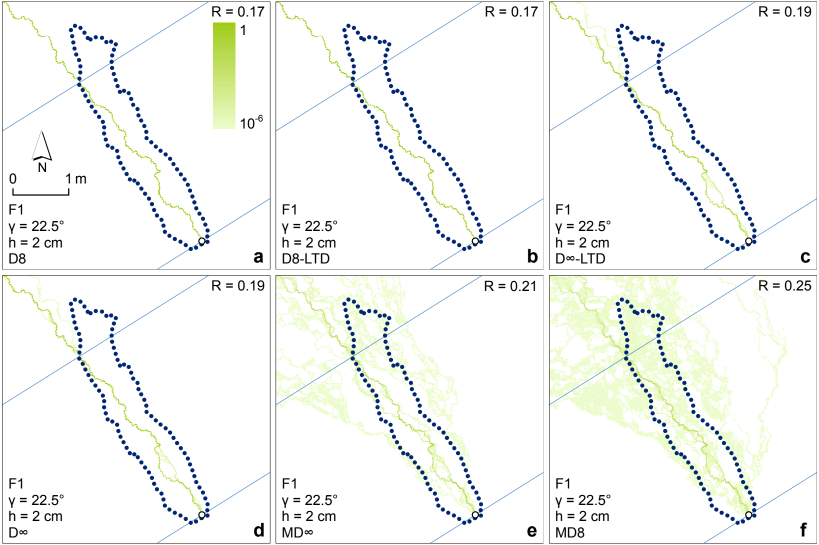

Are predicted flow patterns affected by orientation of grid cells?

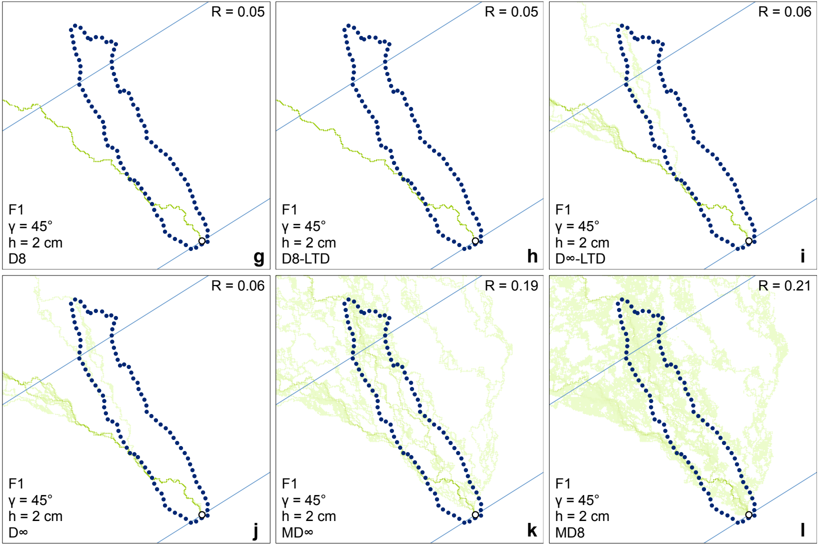

Are predicted flow patterns affected by orientation of grid cells?

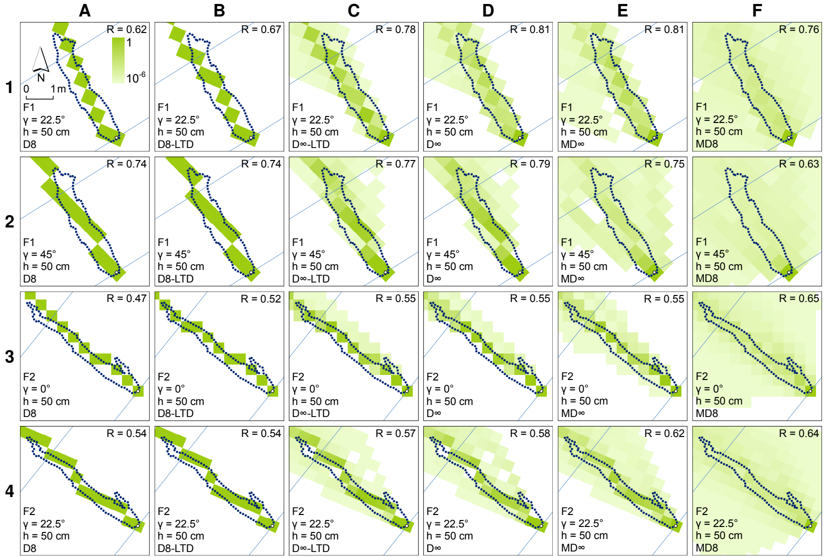

Are predicted flow patterns affected by orientation of grid cells?

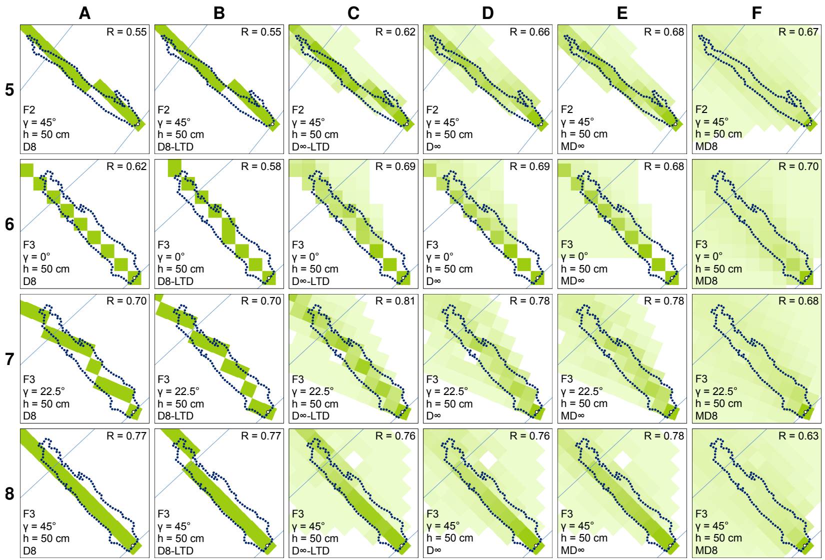

Computational domain.

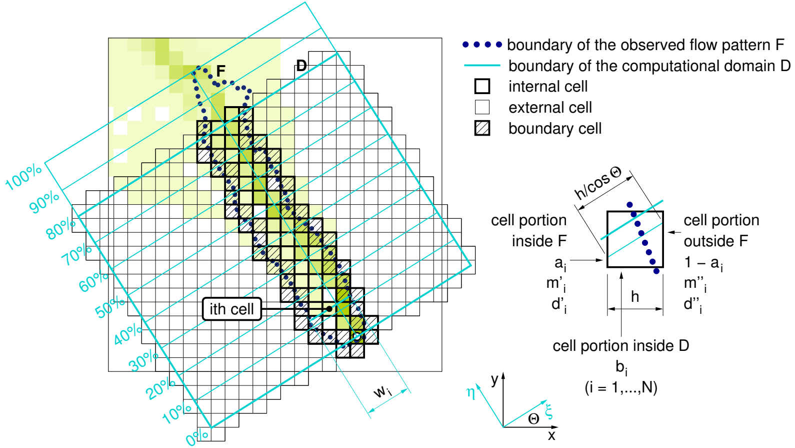

So all you critics sit alone
You're no better than me / for what you've shown.
(Neil Young, Ambulance Blues, On the Beach, 1974)

Predictions and data available for the comparison.

Computational cell

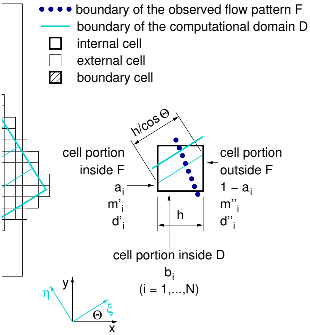

Data

$$M = (m'_1, \ldots, m'_N, m''_1, \ldots, m''_N)$$

$$D = (d'_1, \ldots, d'_N, d''_1, \ldots, d''_N)$$

$$m'_i = m_i \quad (i = 1, \ldots, N)$$

$$m''_i = m_i \quad (i = 1, \ldots, N)$$

$$d'_i = \frac{h/\cos\Theta}{w_i} \quad (i = 1, \ldots, N)$$

$$d''_i = 0 \quad (i = 1, \ldots, N)$$

Weighted Pearson correlation coefficient.

$$R = \frac{\sum_{i=1}^{N} \left[(d_i' - \bar{d})(m_i' - \bar{m})\, a_i + (d_i'' - \bar{d})(m_i'' - \bar{m})(1 - a_i) \right] b_i}{\delta_d\, \delta_m}$$

$$\bar{d} = \sum_{i=1}^{N} \left[d_i'\, a_i + d_i''\, (1 - a_i) \right] b_i \Bigg/ \sum_{i=1}^{N} b_i$$

$$\bar{m} = \sum_{i=1}^{N} \left[m_i'\, a_i + m_i''\, (1 - a_i) \right] b_i \Bigg/ \sum_{i=1}^{N} b_i$$

$$\delta_d = \sqrt{\sum_{i=1}^{N} \left[(d_i' - \bar{d})^2\, a_i + (d_i'' - \bar{d})^2\, (1 - a_i) \right] b_i}$$

$$\delta_m = \sqrt{\sum_{i=1}^{N} \left[(m_i' - \bar{m})^2\, a_i + (m_i'' - \bar{m})^2\, (1 - a_i) \right] b_i}$$

Central tendency and dispersion of correlation coefficients.

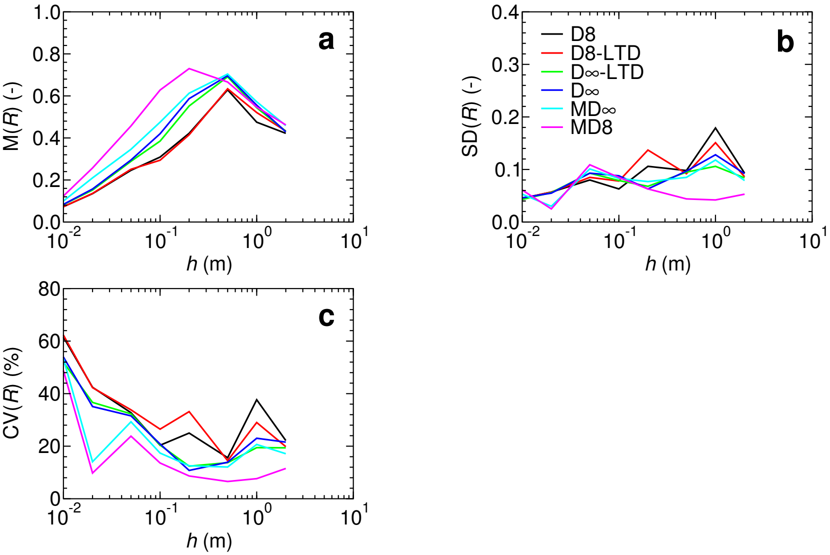

Summary

- Terrestrial laser scanners and thermal imaging cameras can detect overland flow patterns.
- Observed overland flow dispersion rapidly attenuates as flow propagates downslope.
- Grid cell size strongly affects modeled overland flow dispersion.
- All flow direction methods were found to be poorly sensitive when extremely fine grids ($h \leq 2$ cm) were used, and to be poorly specific when coarse grids ($h = 2$ m) were used. Satisfactory results were, however, obtained in grids having resolutions h that approach the average flow width (50 cm), with the best performances displayed by the MD8 method in the finest grids (5 cm $\leq h \leq$ 20 cm), and by the MD∞, D∞, and D∞-LTD methods in the coarsest grids (20 cm $< h \leq$ 1 m).

Directions for future research.

- Sufficiently extended flow patterns have to be experimentally generated, observed, and modeled in order to evaluate the capabilities of terrain analysis methods in distributed catchment models having limited grid resolution ($1\text{ m} \leq h \leq 100\text{ m}$) as a result of computational constraints.
- Scale issues affecting the relation between land surface microtopography, dispersion, and size of grid cells involved need to be investigated to provide a hydrological basis for the description of flow partitioning along the slope directions identified by terrain analysis methods.
- Mixing in overland flows may be studied by generating complex flows from multiple source points or distributed nonpoint sources. This task may be facilitated by using innovative methods for tracing the flow elements within the mixing flows (e.g., Tauro et al., 2012, HESS).

The CATchment HYdrology (CATHY) model.
(Camporese et al., 2010, WRR)

Path-based surface flow analysis

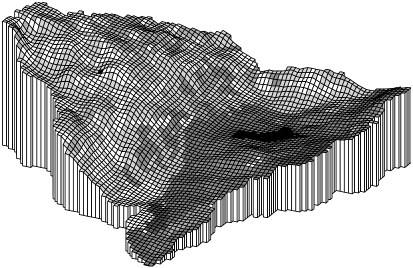

Surface-subsurface flow interaction

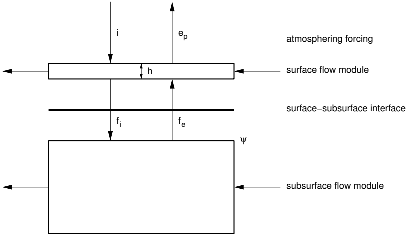

Return

Overland flow phenomenology.
(Raudkivi, 1979, p. 170 and 171)

When the rate of rainfall or snowmelt exceeds the interception requirements and the rate of infiltration, water starts to accumulate on the surface. At first the excess water collects into the small depressions and hollows, until the surface detention requirements are satisfied. After that water begins to move down the slope as a thin film and tiny streams. This early stage of overland flow is greatly influenced by surface tension and friction forces. With continuing rainfall the depth of surface detention and the rate of overland flow increase, but the paths of the small streams on the surface of the catchment are still tortuous and full of obstructions. Every small obstruction causes a delay until the upstream level has risen to overflow the obstacle or to wash it away. On release a small wave speeds downstream and merges with another little rivulet. The merging of more and more of these little streams culminates in the river which drains the whole catchment in question.

Return

Skeleton construction techniques.
(Moretti and Orlandini, 2008, WRR)

Skeleton

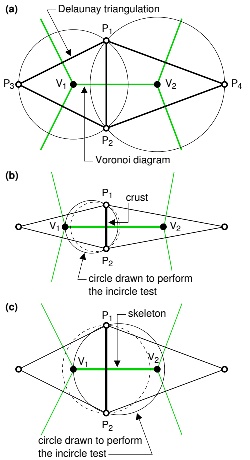

Hipped roof geometry

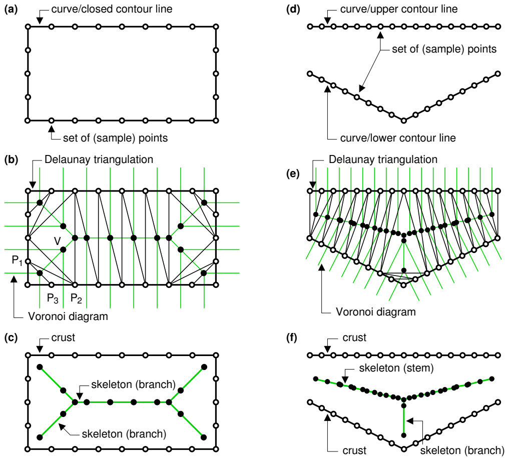

Skeleton construction techniques.
(Moretti and Orlandini, 2008, WRR)

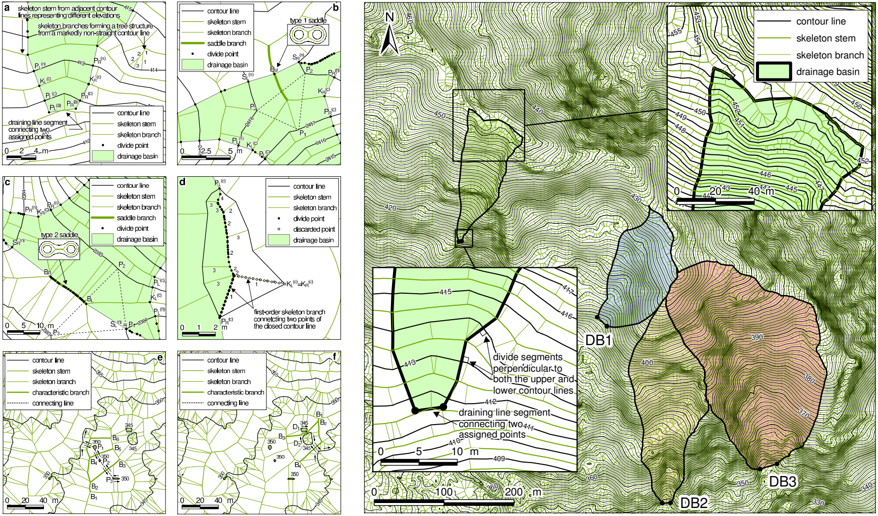

Slope lines.

(Cayley, 1859, London Edinburgh Dublin Philos. Mag. J. Sci.)
(Maxwell, 1870, London Edinburgh Dublin Philos. Mag. J. Sci.)

James Clerk Maxwell

Return

On hills and dales

240 HILLS AND DALES.

If we put L equal to the whole number of lines, and P equal to the whole number of points, we find that F, the number of natural districts named from a hill and a dale together, is equal to W, the number of watersheds or watercourses, or to the whole number of summits, bottoms, passes, and bars diminished by 2.

Chart of an Inland Basin.

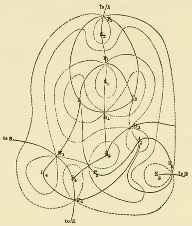

I_1, I_2, I_3, I_4. Lowest points, Bottoms or Immits.
S_1, S_2, S_4, S_5. Highest points, Tops or Summits.
B_1, B_2, B_3. Bars between regions of depression.
P_1, P_2, P_3, P_4, P_5. Passes between regions of elevation.
I_1 B_1 I_2 &c. Lines of Watercourse.
S_1 P_1 S_2 &c. Lines of Watershed.
Dotted line. Contour-lines.

Least Transverse Deviation (LTD).
(Orlandini et al., 2003, WRR)

Path-based analysis

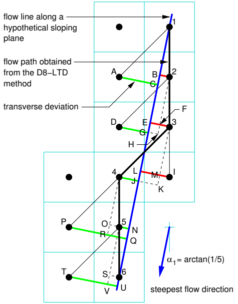

◂ Return

Correction of the nonlocal bias